Biological Psychiatry: Celebrating 50 Years

Archival Report

A Novel Apolipoprotein E Antagonist Functionally Blocks Apolipoprotein E Interaction With N-terminal Amyloid Precursor Protein, Reduces β-Amyloid-Associated Pathology, and Improves Cognition

Darrell Sawmiller, Ahsan Habib, Huayan Hou, Takashi Mori, Anran Fan, Jun Tian, Jin Zeng, Brian Giunta, Paul R. Sanberg, Mark P. Mattson, and Jun Tan

ABSTRACT

BACKGROUND: The ε4 isoform of apolipoprotein E (apoE4) is a major genetic risk factor for the development of sporadic Alzheimer's disease (AD), and its modification has been an intense focus for treatment of AD during recent years.

METHODS: We investigated the binding of apoE, a peptide corresponding to its low-density lipoprotein receptor binding domain (amino acids 133–152; ApoEp), and modified ApoEp to amyloid precursor protein (APP) and their effects on amyloid-β (Aβ) production in cultured cells. Having discovered a peptide (6KApoEp) that blocks the interaction of apoE with N-terminal APP, we investigated the effects of this peptide and ApoEp on AD-like pathology and behavioral impairment in 3XTg-AD and 5XFAD transgenic mice.

RESULTS: ApoE and ApoEp, but not truncated apoE lacking the low-density lipoprotein receptor binding domain, physically interacted with N-terminal APP and thereby mediated Aβ production. Interestingly, the addition of 6 lysine residues to the N-terminus of ApoEp (6KApoEp) directly inhibited apoE binding to N-terminal APP and markedly limited apoE- and ApoEp-mediated Aβ generation, presumably through decreasing APP cellular membrane trafficking and p44/42 mitogen-activated protein kinase phosphorylation. Moreover, while promoting apoE interaction with APP by ApoEp exacerbated Aβ and tau brain pathologies in 3XTg-AD mice, disrupting this interaction by 6KApoEp ameliorated cerebral Aβ and tau pathologies, neuronal apoptosis, synaptic loss, and hippocampal-dependent learning and memory impairment in 5XFAD mice without altering cholesterol, low-density lipoprotein receptor, and apoE expression levels.

CONCLUSIONS: These data suggest that disrupting apoE interaction with N-terminal APP may be a novel disease-modifying therapeutic strategy for AD.

Keywords: Acetylated and phosphorylated tau, Alzheimer's disease, Alzheimer's mouse model, Amyloid precursor protein, Amyloidogenesis, Apolipoprotein E, Low-density lipoprotein receptor binding domain

https://doi.org/10.1016/j.biopsych.2019.04.026

Affecting as many as 47 million people worldwide, Alzheimer's disease (AD) is characterized by the accumulation of amyloid-β (Aβ) plaques and neurofibrillary tangles in the brain (1–4). Aβ is produced via β- and γ-secretase-mediated proteolysis of amyloid precursor protein (APP) (5,6), a type I transmembrane protein, which can then aggregate to form plaques. According to the amyloid hypothesis, overproduction of Aβ triggers neuronal apoptosis (7,8), inflammation (9,10), oxidative stress (11,12), and tau phosphorylation and aggregation in intracellular neurofibrillary tangles (13). While inherited early-onset familial AD results from mutations in *APP* or presenilin genes, in the more common late-onset sporadic AD, excess Aβ generation is enhanced by age-related factors, metabolic dysfunction, cardiovascular disease, and brain injury (14–16). In addition, the apoE4 isoform of apolipoprotein E (apoE) has been found to be the major genetic risk factor for the development of sporadic AD (17). Recently, because several therapeutic approaches targeting Aβ have failed, the relevance of Aβ in the AD pathogenesis has been questioned.

ApoE, a major component of chylomicron remnants and very-low-, intermediate-, and high-density peripheral- and brain-derived lipoproteins, plays an important role in receptor-mediated cholesterol endocytosis (18,19). The cause of the increased risk for AD associated with the presence of apoE4

SEE COMMENTARY ON PAGE 169

 ISSN: 0006-3223

may involve enhanced formation and reduced clearance of Aβ (20,21), the formation of neurotoxic apoE4 peptide fragments (22,23), abnormal tau phosphorylation, neuroinflammation, and neurodegeneration (24–27). An early study using the yeast two-hybrid system and immunoprecipitation (IP) suggested that the N-terminal APP can directly bind to apoE, thereby enhancing intracellular APP endocytosis and reducing soluble APPα (sAPPα) production (28). A more recent study indicates that both glia-derived apoE and recombinant apoE stimulate Aβ production in human neurons with a rank order of potency of apoE4 > apoE3 > apoE2, mediated by activation of a noncanonical mitogen-activated protein kinase (MAPK) p44/42 and enhanced transcription/translation of APP (29). These studies suggest that apoE directly binds to the N-terminal region of APP, thereby enhancing APP endocytosis and directing its processing from sAPPα to Aβ. Recently, we further explored the binding of apoE to the N-terminal APP in Aβ production and generated a novel peptide antagonist of this interaction that reduced Aβ production and pathology in AD mouse models. Taken together, our results suggest that disruption of apoE interaction with the N-terminal APP may be a novel disease-modifying therapeutic strategy for AD.

METHODS AND MATERIALS

Cell Culture

Chinese hamster ovary (CHO) cells engineered to express human wild-type APP (CHO/APPwt) or Swedish mutant APP (CHO/APPswe) were cultured in 96- or 24-well plates at 4×10^4 or 2×10^5 cells/well, respectively, in Dulbecco's modified Eagle's medium with fetal bovine serum (10%), 1 mM sodium pyruvate, and 100 U/mL penicillin/streptomycin. In addition, SH-SY5Y cells transfected with APPswe and wild-type SH-SY5Y cells were cultured as described previously (30). Primary hN2^{TM} human neurons were cultured in hN2^{TM} human neuron culture medium, and primary HCN2 human neurons were cultured in Dulbecco's modified Eagle's medium with 4 mM

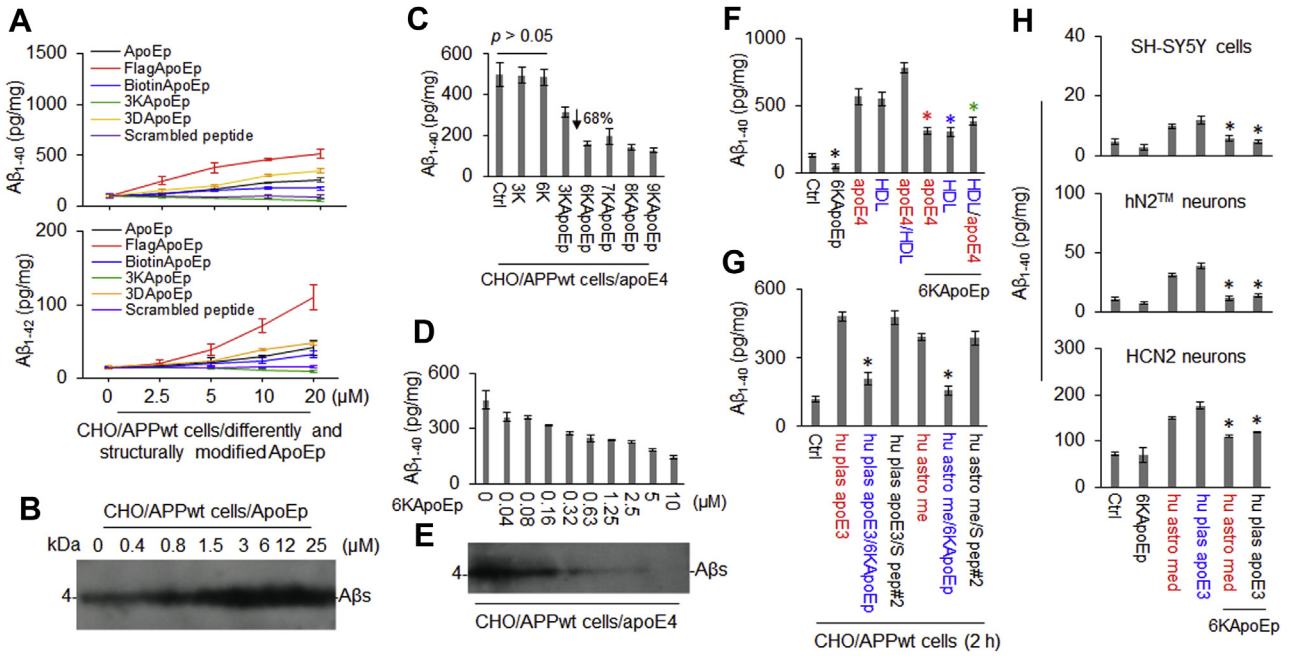

Figure 1. A novel apolipoprotein E antagonist (6KapoEp), consisting of the apoE low density lipoprotein receptor binding domain (ApoEp) with 6 lysine residues attached at the N-terminus, markedly inhibits human recombinant and lipidated apoE-mediated amyloid-β (Aβ) production. **(A, B)** Chinese hamster ovary/wild-type amyloid precursor protein (CHO/APPwt) cells were treated with ApoEp, FlagApoEp, BiotinApoEp, 3K (3 lysine residues) ApoEp, 3D (3 aspartate residues) ApoEp, or scrambled peptide at 0 to 25 μM, followed after 2 hours by analysis of Aβ levels in conditioned media by Aβ enzyme-linked immunosorbent assay (ELISA) **(A)** and after 16 hours by analysis of Aβ in cell lysates by Western blot using 82E1 antibody **(B)**. **(C–E)** In addition, CHO/APPwt cells were treated with phosphate-buffered saline control (Ctrl) or 3K, 6K, 3KApoEp, 6KApoEp, 7KApoEp, 8KApoEp, or 9KApoEp at 10 μM, or with 6KApoEp at 0 to 10 μM, for 15 minutes, followed by the addition of human recombinant apoE4 (apoE4) at 10 μg/mL and then Aβ ELISA (2 hours) **(C, D)** and Western blot (16 hours) **(E)**. **(F–H)** CHO/APPwt cells, SH-SY5Y neuroblastoma cells, hN2^{TM} human neurons, and HCN2 cortical neurons were also treated with apoE4, human plasma–derived high-density lipoprotein (HDL), or human plasma–derived apoE3 (hu plas apoE3) at 10 μg/mL, apoE4 preincubated with HDL for 1 hour at 37°C (apoE4/HDL), or human astrocyte–derived media (hu astro med) at 1:4 dilution in the absence or presence of 6KApoEp or scrambled peptide (S pep#2) at 10 μM, followed by Aβ ELISA. Preincubating with HDL has been previously reported to lipidate apoE (48). Hu astro med was obtained from human astrocytes (CCF-STTG1/ATCC CRL-1718) as described previously (49). ELISA results are representative of three independent experiments, with each condition duplicated and presented as the mean ± SD of Aβ (pg/mg total intracellular protein). Asterisk indicates $p < .05$ for ApoEp-, FlagApoEp-, BiotinApoEp-, or 3DApoEp-mediated Aβ production, compared with scrambled peptide (#1)- or 3KApoEp-mediated Aβ production, as determined by one-way analysis of variance **(A)**, and apoE4-, hu plas apoE3-, or hu astro media-mediated Aβ production in the presence of 6KApoEp, compared with the absence of 6KApoEp, as determined by *t* test **(F–H)**.

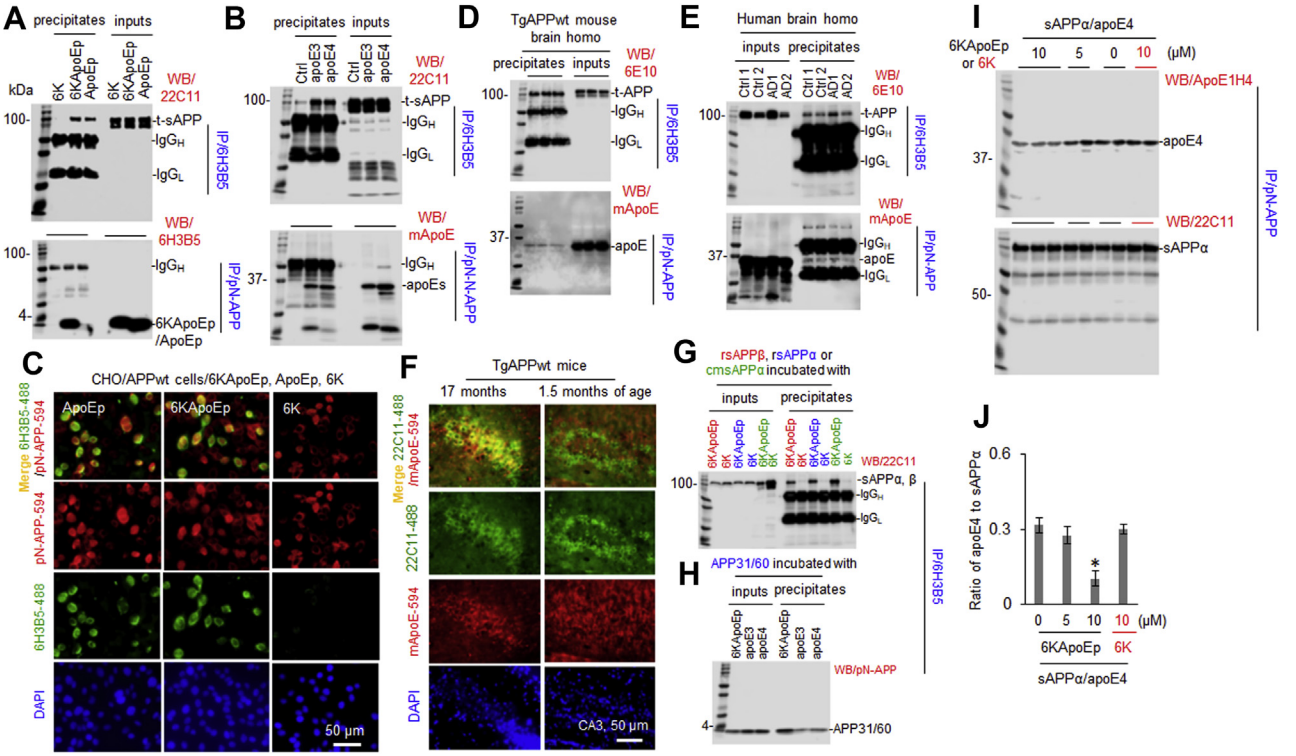

Figure 2. Apolipoprotein E antagonist (6KApoEp) physically interacts with N-terminal amyloid precursor protein (APP). **(A, B)** Chinese hamster ovary/wild-type APP (CHO/APPwt) cells were treated with 6KApoEp, ApoEp, or 6K at 10 μM **(A)**, apolipoprotein E3 (apoE3) or apoE4 at 10 μg/mL, or phosphate-buffered saline control (Ctrl) **(B)** for 2 hours, followed by immunoprecipitation (IP) of the conditioned media with mouse monoclonal anti-apoE low-density lipoprotein receptor binding domain antibody (6H3B5) or rabbit polyclonal anti-N-terminal APP41/66 antibody (pN-APP). Total secreted APP (t-sAPP), 6KApoEp, ApoEp, apoE3, and apoE4 in total conditioned media (inputs) and immunoprecipitates (precipitates) were then determined by Western blot (WB) using mouse anti-N-terminal APP antibody (22C11), 6H3B5, and rabbit anti-human apoE antibody (mApoE) **(A, B)**. **(C)** CHO/APPwt cells were also plated at 8-well chambers at 1×10^5/well for 24 hours, treated with 6K, ApoEp, or 6KApoEp at 10 μM for 2 hours, fixed in 4% paraformaldehyde solution, and stained with 6H3B5 and pN-APP. Alexa Fluor 488 goat anti-mouse immunoglobulin G (IgG) was used to detect ApoEp and 6KApoEp (green), while Alexa Fluor 594 donkey anti-rabbit IgG was used to detect N-terminal APP (red). DAPI (4′,6-diamidino-2-phenylindole) costaining showed nuclear DNA. **(D, E)** Brain tissue homogenates prepared from three TgAPPwt mice (two female and one male), two patients with Alzheimer's disease (AD1 [male] and AD2 [female]), and two normal age-matched control cortices (Ctrl1 [male] and Ctrl2 [female]) were immunoprecipitated with 6H3B5 or pN-APP, and t-APP and apoE were determined by WB analysis using 6E10 and mApoE, respectively. **(F)** Brain tissue sections from aged and young TgAPPwt mice (two for each group [one female and one male]) were also stained with 22C11 and mApoE at 4°C overnight, followed by staining with Alexa Fluor 488 goat anti-mouse IgG to detect cell surface APP (green) and with Alexa Fluor 594 donkey anti-rabbit IgG to detect apoE (red). **(G, H)** As in vitro confirmation, human recombinant sAPPβ (rsAPPβ, without Aβ domain), rsAPPα, CHO/APPwt cell conditioned media–derived sAPPα (cmsAPPα), or APP N-terminal peptide (amino acids 31–60; APP31/60) at 100 nM was incubated with 6KApoEp, 6K, apoE3, or apoE4 at 100 nM at 37°C for 1 hour, followed by IP with 6H3B5. sAPPα/β and APP31/60 in total (inputs) and immunoprecipitates were determined by WB analysis using 22C11 and pN-APP, respectively. **(I)** In addition, human sAPPα protein at 100 nM was also incubated with apoE4 protein at 100 nM in the absence or presence of 6KApoEp or 6K at 5 or 10 μM for 1 hour at 37°C, followed by IP with pN-APP and determination of apoE4 and sAPPα in precipitates by WB analysis using ApoE1H4 and 22C11. **(J)** Band density ratios of apoE4 to total sAPPα were determined by densitometry analysis. The results shown in panel **(J)** are representative of two independent experiments, with each condition duplicated. Asterisk indicates $p < .05$ compared with the controls as determined by *t* test. Overall, 6KApoEp, ApoEp, apoE3, and apoE4, but not 6K, were immunoprecipitated and localized with N-terminal APP in vitro and in vivo. ApoE was colocalized with N-terminal APP more in aged TgAPPwt mouse brains compared with young TgAPPwt mouse brains. 6KApoEp, but not 6K, reduced coimmunoprecipitation of sAPPα with apoE4. The AD patient and age-matched control cortices were provided by Banner Sun Health Research Institute (Sun City, AZ). The results shown in panels (**A–D**) are representative of two or three independent experiments. IgGH and IgGL, immunoglobulin heavy and light chain.

L-glutamine adjusted to contain 1.5 g/L sodium bicarbonate, 4.5 g/L glucose, and fetal bovine serum (10%).

Enzyme-Linked Immunosorbent Assay, Western Blotting, and IP

$A\beta_{1-40,42}$ and sAPPα from cell cultures and brain homogenates were detected by Aβ and sAPPα enzyme-linked immunosorbent assay kits (IBL America, Minneapolis, MN), strictly following the manufacturer's instructions (31,32). Western blotting (WB) analyses were performed as described previously (31,32). IP was performed by first incubating conditioned medium or cell lysates with appropriate antibodies and Protein-A/G Mag Sepharose beads (GE Healthcare Life Sciences, Pittsburgh, PA) overnight with gentle rocking at 4°C, followed by three washes with binding buffer (50 mM Tris and 150 mM NaCl, pH 7.5) and analysis by WB. The effect of apoE4 and 6KApoEp, an apoE antagonist consisting of the apoE low density lipoprotein receptor (LDLR) binding domain with 6 lysine residues added at its N-terminus, on cell surface

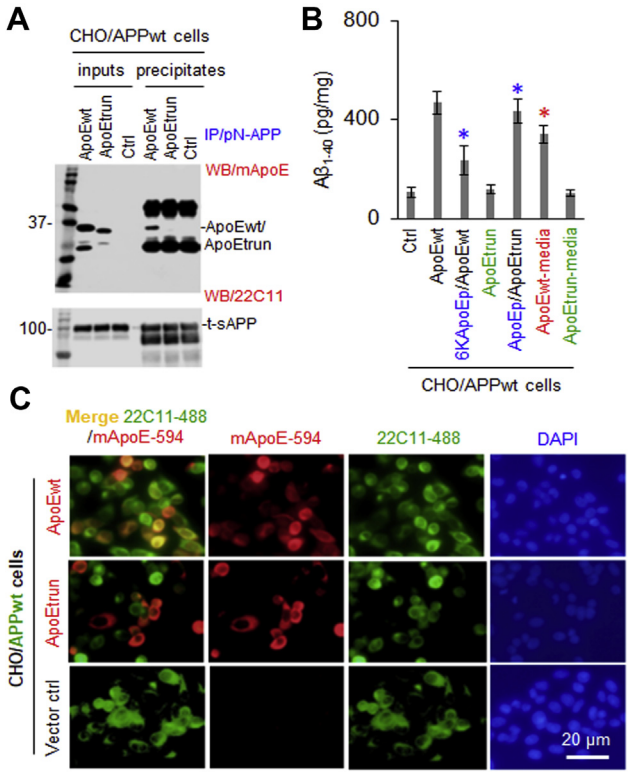

Figure 3. Truncated apolipoprotein E (apoE) lacking the low-density lipoprotein receptor binding domain failed to promote amyloid-β (Aβ) production in Chinese hamster ovary/wild-type amyloid precursor protein (CHO/APPwt) cells. **(A)** Conditioned media collected from CHO/APPwt cells cotransiently expressing human wild-type apoE4 (CHO/APPwt/ApoEwt), truncated apoE4 lacking the low-density lipoprotein receptor binding domain (CHO/APPwt/ApoEtrun), or control vector (CHO/APPwt/Ctrl) were immunoprecipitated (IP) with anti-N-terminal APP41/66 antibody (pN-APP) and then apoE and total secreted APP (t-sAPP) in total conditioned media (inputs), and immunoprecipitates (precipitates) were determined by Western blot (WB) analysis using rabbit monoclonal anti-apoE antibody (mApoE) and mouse monoclonal anti-N-terminal APP (22C11), respectively. **(B)** In addition, CHO/APPwt/ApoEwt, CHO/APPwt/ApoEtrun, and CHO/APPwt/Ctrl cells were cultured on 24-well plates at 1×10^5/well overnight and then treated with apoE antagonist (6KApoEp) or ApoEp at 10 μM, and CHO/APPwt/Ctrl cells were treated with conditioned media collected from CHO/APPwt/ApoEwt or CHO/APPwt/ApoEtrun cells, for 2 hours followed by Aβ enzyme-linked immunosorbent assay. **(C)** Furthermore, CHO/APPwt/ApoEwt, CHO/APPwt/ApoEtrun, or CHO/APPwt/Ctrl cells were also plated in 8-well chambers at 1×10^5/well for 24 hours, fixed in 4% paraformaldehyde solution, and stained with 22C11 and mApoE. Alexa Fluor 488 goat anti-mouse immunoglobulin G was used to detect cell surface APP (green), while Alexa Fluor 594 donkey anti-rabbit immunoglobulin G was used to detect apoE (red). ApoEwt but not ApoEtrun was coimmunoprecipitated **(A)** and colocalized with cell surface APP (**C**, left panels merged) and enhanced Aβ production **(B)**, indicating that the low-density lipoprotein receptor binding domain is necessary for apoE interaction with the N-terminal APP. Notably, 6KApoEp markedly reduced Aβ production in CHO/APPwt/ApoEwt cells, while ApoEp significantly restored Aβ production in CHO/APPwt/ApoEtrun cells **(B)**. Enzyme-linked immunosorbent assay results are representative of three independent experiments, with each condition duplicated and presented as the mean ± SD of Aβ (pg/mg total intracellular protein). Asterisk indicates $p < .05$ for Aβ production in the presence of 6KApoEp or ApoEp compared with the corresponding absence of 6KApoEp or ApoEp or in the presence of CHO/APPwt/ApoEwt compared with CHO/APPwt/ApoEtrun media as determined by *t* test. DAPI, 4′,6-diamidino-2-phenylindole.

expression of APP, LDLR, and LDLR-related protein 1 (LRP1) was determined by biotinylation and avidin precipitation as described previously (33).

Real-Time Polymerase Chain Reaction

Total RNA was extracted from CHO/APPwt cells after treatment with 6KApoEp using an RNeasy Plus Mini Kit (Qiagen, Germantown, MD). The purity and concentration of RNA was quantified using a NanoDrop 2000c spectrophotometer (Thermo Fisher Scientific, Waltham, MA). The quantification of target RNAs was performed in a total volume of 50 μL by real-time one-step reverse transcription–quantitative polymerase chain reactions (10 ng RNA, 250 mM forward and reverse primers) using SYBR Green I in an IQ5 multicolor real-time polymerase chain reaction detection system (Bio-Rad, Hercules, CA) according to manufacturer's instructions. RNA primers were designed to selectively amplify and quantify human APP and LDLR and CHO cell β-actin (IDT, Coralville, IA) as indicated.

Cholesterol Quantitation

For determination of CHO/APPwt cell–associated cholesterol levels, cells were washed three times with ice-cold phosphate-buffered saline (PBS), lysed by sonication in chloroform:isopropanol:IGEPAL CA-630 (7:11:0.1), and centrifuged. The organic phase was air-dried at 50°C to remove chloroform and diluted 10-fold in the cholesterol assay buffer for the cholesterol determination by a fluorometric cholesterol quantitation kit (MilliporeSigma, Burlington, MA) according to the manufacturer's instructions.

Mice

All mice were housed and maintained in the Morsani College of Medicine Animal Facility at the University of South Florida, and all experiments were conducted in compliance with protocols approved by the University of South Florida Institutional Animal Care and Use Committee. 5XFAD mice at 6 weeks of age (n = 10; 5 female and 5 male) were intraperitoneally treated with 6KApoEp (250 μg/kg in 50 μL PBS) or PBS (50 μL) daily for 12 weeks. 3XTg-AD mice at 9 months of age (n = 6; 3 female and 3 male) were intraperitoneally treated with ApoEp (250 μg/kg in 50 μL PBS) or PBS (50 μL) daily for 12 weeks. After 11 weeks of treatment, 5XFAD mice were subjected to the Y maze, fear conditioning, novel object recognition, and open field behavioral testing as described previously (34,35).

After treatment and behavioral testing, all mice were anesthetized with 2% to 4% isoflurane (MilliporeSigma), followed by collection of blood, euthanization by bilateral thoracotomy, transcardial perfusion with physiological saline-containing heparin (10 U/mL; MilliporeSigma), and isolation of the brain for biochemistry, immunohistochemistry (IHC), and immunofluorescence (IF) analyses. Briefly, one hemisphere was frozen immediately in liquid nitrogen and stored at −80°C, followed by sonication in RIPA buffer (Cell Signaling Technology, Danvers, MA) containing protease inhibitor and phosphatase inhibitor cocktail (Thermo Fisher Scientific), centrifugation, and WB analysis of the supernatant. The other hemisphere was placed in 4% paraformaldehyde in PBS for cryostat sectioning. The 25-μm free-floating coronal sections were collected and stored in PBS with 100 mM sodium azide at 4°C for IHC and IF analyses.

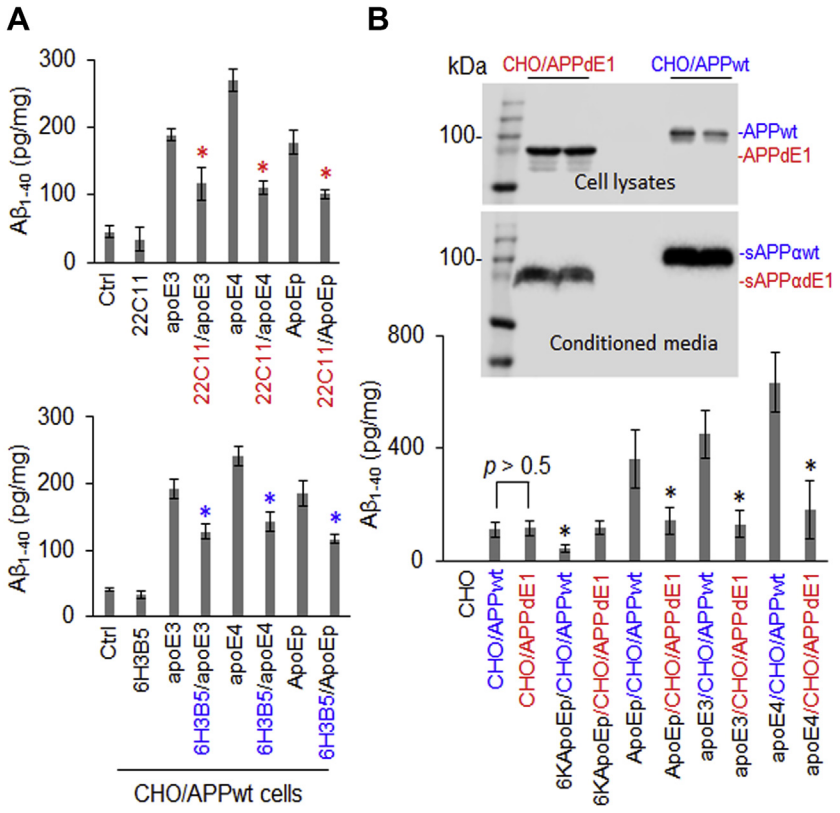

Figure 4. Apolipoprotein E (apoE)-promoted amyloid-β (Aβ) production was significantly attenuated by specific antibodies against the apoE low-density lipoprotein receptor (LDLR) binding domain or the N-terminal amyloid precursor protein (APP) or by expression of N-terminally truncated APP. **(A)** Chinese hamster ovary/wild-type APP (CHO/APPwt) cells were treated with apoE3 or apoE4 at 10 μg/mL or with ApoEp (a peptide corresponding to apoE's LDLR binding domain) at 5 μM in the absence or presence of anti-N-terminal APP (22C11) or anti-apoE LDLR binding domain antibody (6H3B5) at 10 μg/mL for 2 hours, followed by Aβ enzyme-linked immunosorbent assay (ELISA). **(B)** CHO cells were also transfected with pCMV6 APP695 or pCMV6 E1–depleted APP695, yielding cells expressing wild-type APP695 (CHO/APPwt) or truncated APP695 lacking the N-terminal E1 region (CHO/APPdE1). After 24 hours, the cells were treated with apoE antagonist (6KApoEp) or ApoEp at 10 μM, or apoE3 or apoE4 at 10 μg/mL, for 3 hours, followed by Aβ ELISA (lower panel). APPwt/dE1 in cell lysates and sAPPαwt/dE1 in conditioned media derived from the transfected CHO cells were determined by Western blot analysis using 6E10 (upper panels). ApoE3-, apoE4-, and ApoEp-mediated Aβ production was markedly reduced by 22C11, 6H3B5, and truncation of the dE1 region of APP, indicating that apoE-mediated Aβ production is mediated by interaction of apoE LDLR binding domain with N-terminal APP. Isotype-matched control immunoglobulin G failed to reduce apoE3-, apoE4-, or ApoEp-mediated Aβ production (data not shown). ELISA results are representative of three independent experiments, with each condition triplicated and presented as the mean ± SD of Aβ (pg/mg total intracellular protein). Asterisk indicates $p < .05$ compared with the corresponding absence of 22C11 or 6H3B5 or the corresponding CHO/APPwt cells as determined by one-way analysis of variance.

IHC and IF

Brain sections from 5XFAD and 3XTg-AD mice were stained with biotin anti-$A\beta_{17-24}$ monoclonal antibody (4G8), VECTASTAIN Elite ABC Kit (Vector Laboratories, Burlingame, CA), and diaminobenzidine substrate, followed by quantitative image analysis of Aβ burden, as described previously (31,32). In addition, brain coronal sections were analyzed by IHC staining with antiacetylated tau (K^{174} and K^{274}) and antiphosphorylated tau (Thr^{231}, Thr^{181}, Thr^{404}, and Ser^{202}/Thr^{205}) antibodies and IF staining with anti-β-tubulin III, anti–neuronal nuclei, anti-cleaved caspase-3, anti-synapsin I, anti-apoE, and anti-N-terminal APP antibodies. For thioflavin S staining, free-floating brain tissue sections mounted on slides were washed in double-distilled water, stained in 1% filtered thioflavin S for 5 minutes, and differentiated in 70% alcohol. For all cell culture and brain tissue staining analyses, images were taken by a BX60 microscope with an attached charge-coupled device camera system (DP72; Olympus, Tokyo, Japan) or using an Olympus FV1000 laser scanning confocal microscope.

Statistical Analysis

All data were normally distributed. Therefore, in instances of single mean comparisons, Levene's test for equality of variances followed by *t* test for independent samples was used to assess significance. In instances of multiple mean comparisons, analysis of variance was used, followed by post hoc comparison using Bonferroni's method. Alpha levels were set at .05 for all analyses. SPSS release 23.0 (IBM, Armonk, NY) was used for all data analyses.

RESULTS

6KApoEp Treatment Markedly Suppresses Human Recombinant and Lipidated apoE-Induced Aβ Production

Previous findings suggest that apoE4 might exacerbate AD pathology, in part, by enhancing APP amyloidogenic processing (29). In addition, the N-terminal region of apoE (residues 133–152) is known to contain the apoE receptor binding domain, while structural modifications of apoE are known to mediate differential interaction of apoE isoforms with its receptor (21). To determine the specific region of apoE mediating Aβ production and further investigate the effects of structural modifications of apoE, we focused on the apoE LDLR binding domain and proximal structural modifications. As expected, an apoE peptide (ApoEp), consisting only of the LDLR binding domain of apoE (residues 133–152), markedly increased Aβ production in a concentration-dependent manner in CHO cells engineered to stably overexpress human wild-type APP (CHO/APPwt

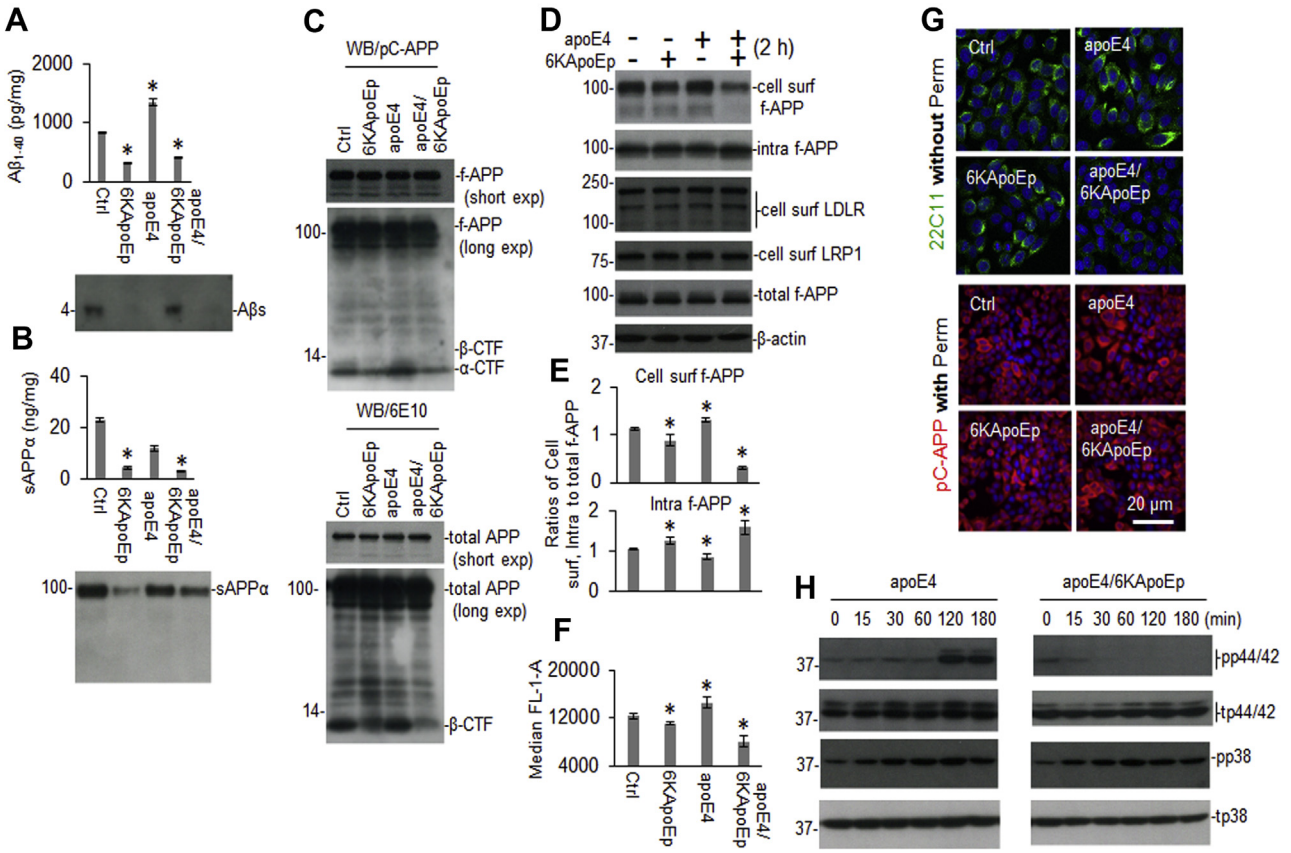

Figure 5. Apolipoprotein E (apoE) antagonist (6KApoEp) inhibits amyloid precursor protein (APP) trafficking to the cell surface and markedly mitigates p44/42 mitogen-activated protein kinase phosphorylation induced by apoE. **(A, B)** Chinese hamster ovary/wild-type APP cells were treated with phosphate-buffered saline control (Ctrl), 6KApoEp at 10 μM, apoE4 at 10 μg/mL, or 6KApoEp and apoE4 for 2 hours, followed by amyloid-β (Aβ) and secreted APPα (sAPPα) enzyme-linked immunosorbent assay (upper panels) and Western blot (WB) analysis using 82E1 and 2B3 antibodies, respectively (lower panels). **(C)** In addition, full-length APP (f-APP, short and long exposure [exp]), α/β-C-terminal fragment (α/β-CTF) and total APP in cell lysates were also analyzed by WB using anti-C-terminal APP750/70 (pC-APP) (upper panel) and anti-N-terminal APP antibody (6E10) (lower panel). **(D)** Cell lysates were biotinylated and immunoprecipitated using Neutravidin beads, and intracellular proteins obtained by Neutravidin depletion (intra) and cell surface proteins obtained by Neutravidin precipitation (cell surf) were analyzed for f-APP, low-density lipoprotein receptor (LDLR), and LDLR-related protein 1 by WB using 6E10, anti-LDLR, and anti-LDLR-related protein 1 antibodies. **(E)** Band density ratios of cell surf or intra to total f-APP were determined by densitometry analysis. **(F)** Cellular membrane–associated full-length APP was analyzed by flow cytometry and is presented as the mean ± SD median fluorescence parameter 1-A (FL-1-A). **(G)** Cultured cells were stained with mouse anti-N-terminal APP (22C11) and rabbit anti-C-terminal APP (pC-APP) primary antibodies after permeabilization (Perm; 0.05% Triton X-100 for 5 minutes) or directly (without Perm) and were observed using an Olympus FV1000 laser scanning confocal microscope. Alexa Fluor 594 donkey anti-rabbit immunoglobulin G and Alexa Fluor 488 goat anti-mouse immunoglobulin G were used to detect APP. **(H)** In addition, Chinese hamster ovary/wild-type APP cells were treated with apoE4 at 10 μg/mL in the absence or presence of 6KApoEp at 10 μM for 0 to 180 minutes, followed by determination of total p44/42 (tp44/42), tp38, phosphorylated p44/42 (pp44/42), and pp38 mitogen-activated protein kinase levels in cell lysates by WB analysis. Enzyme-linked immunosorbent analysis results are representative of three independent experiments, with each condition triplicated and presented as the mean ± SD. Asterisk indicates $p < .05$ compared with Ctrl as determined by *t* test.

cells) (Figure 1A, B and Supplemental Figure S1A). Interestingly, while N-terminal addition of Flag-tag greatly enhanced the efficacy of ApoEp to increase $A\beta_{1-40,42}$ levels, the addition of three lysine residues terminated this amyloidogenic effect (Figure 1A).

To test the hypothesis that the addition of N-terminal lysine residues might convert ApoEp to an apoE antagonist, we examined the effects of ApoEp containing 3, 6, 7, 8, or 9 lysine residues on apoE4-induced Aβ production. 3KApoEp moderately reduced, while 6K- to 9KApoEp markedly and maximally reduced, both basal and apoE4-induced Aβ production (Figure 1C and Supplemental Figure S1B–D). In addition, 6KApoEp reduced apoE4-induced Aβ production in a concentration-dependent fashion, starting at 40 nM and with an IC_{50} of approximately 0.32 to 0.63 μM (Figure 1D, E and Supplemental Figure S1C). This reduction was observed regardless of whether the cells were cotreated with 6KApoEp together with apoE4, pretreated with 6KApoEp, or treated with apoE4 preincubated with 6KApoEp (Supplemental Figure S3). 6KApoEp also reduced Aβ production elicited by high-density lipoprotein (HDL)-lipidated apoE4, human plasma–derived apoE3, and human astrocyte media–derived apoE in CHO/APPwt and SH-SY5Y human neuroblastoma cells as well as hN2^{TM} and HCN2 human neurons (Figure 1F–H), confirming that 6KApoEp reduces natural apoE-mediated Aβ production.

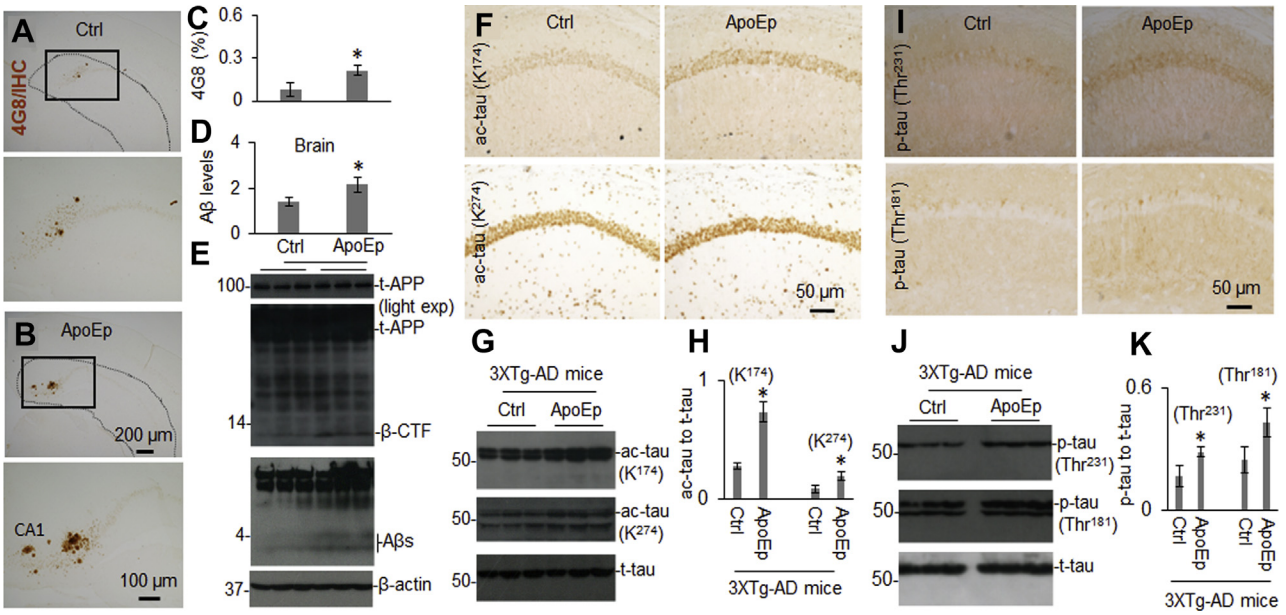

Figure 6. Peripheral administration of apolipoprotein E peptide (ApoEp) significantly enhances β-amyloid- and tau-associated pathologies. **(A, B)** Six 3XTg-AD mice (3 female and 3 male) at 9 months of age were treated with ApoEp at 250 μg/kg or vehicle control (Ctrl; phosphate-buffered saline alone) intraperitoneally daily for 12 weeks. Following sacrifice, amyloid-β (Aβ) in brain coronal sections was analyzed by immunohistochemistry staining using 4G8 antibody. **(C)** Percentage of Aβ immunoreactive plaques from hippocampus and cortex was quantified by densitometry analysis. **(D, E)** In addition, $Aβ_{1–40,42}$ levels in brain homogenates were analyzed by enzyme-linked immunosorbent assay **(D)** and total amyloid precursor protein (t-APP), β-C-terminal fragment (β-CTF), and soluble total Aβ (Aβs) were determined by Western blot analysis using 6E10 (t-APP and β-CTF) and 82E1 (Aβs) **(E)**. **(F–K)** Acetylated tau (ac-tau; K^{174} and K^{274}) and phosphorylated tau (p-tau; Thr^{231} and Thr^{181}) were determined by immunohistochemistry staining **(F, I)** and Western blot analyses **(G, J)**. Band density ratios of acetylated or phosphorylated tau to total tau were determined by densitometry analysis **(H, K)**. Asterisk indicates $p < .05$ compared with Ctrl. Enzyme-linked immunosorbent assay results and band density ratios are represented as the mean ± SD. light exp, light exposure.

6KApoEp Reduces Physical Association of apoE With N-Terminal APP

Previously, apoE was found to bind to the N-terminal APP, upstream of the Aβ region, and thereby enhances APP endocytosis and reduces sAPPα production (28). To confirm this physical association of apoE with N-terminal APP, CHO/APPwt cells were treated with ApoEp, 6KApoEp, 6K, apoE3, or apoE4 followed by IP of apoE with anti-LDLR binding domain antibody (6H3B5). Total secreted APP in conditioned media and full-length APP in cell lysates were then determined by WB analysis using anti-N-terminal (22C11) and anti-C-terminal APP (pC-APP) antibodies, respectively. Alternatively, N-terminal APP was immunoprecipitated with anti-N-terminal APP41/66 (pN-APP) antibody followed by analysis of apoE, 6KApoEp, and ApoEp using anti-human apoE (mApoE) and 6H3B5 antibodies. ApoE, ApoEp, and 6KApoEp were coimmunoprecipitated with secreted APP in conditioned media and full-length APP in cell lysates (Figure 2A, B and Supplemental Figure S2A–C). In addition, ApoEp and 6KApoEp were colocalized with N-terminal APP in cultured CHO/APPwt cells, as determined by IF staining with 6H3B5 and pN-APP antibodies (Figure 2C), respectively, confirming that N-terminal APP physically associates with apoE in vitro. ApoE also coimmunoprecipated with N-terminal APP in homogenates prepared from brains of TgAPPwt mice, patients with AD, and age-matched control subjects, confirming that the physical association of apoE with N-terminal APP occurs in vivo (Figure 2D, E). Most interesting, apoE was colocalized with cell surface APP more in brains from aged TgAPPwt mice compared with young TgAPPwt mice, suggesting an age-associated increase in apoE–N-terminal APP interaction (Figure 2F). However, WB analysis showed no significant differences in total apoE and APP levels between young and aged TgAPPwt mouse brain homogenates (data not shown).

As in vitro confirmation of physical association of apoE with N-terminal APP, human recombinant sAPPβ (without Aβ domain), sAPPα, CHO/APPwt-conditioned media-derived sAPPα, or APP N-terminal peptide (amino acids 31–60; APP31/60) was incubated with 6KApoEp, 6K, apoE3, or apoE4 followed by IP of apoE LDLR binding domain with 6H3B5 and WB analysis of sAPPα/β and APP31/60 (Figure 2G, H). Human recombinant sAPPα protein was also incubated with apoE4 in the absence or presence of 6KApoEp or 6K followed by IP with pN-APP and WB analysis of apoE and sAPPα (Figure 2I, J). Overall, sAPPα/β and APP31/60 were coimmunoprecipitated with 6KApoEp and apoE in vitro, confirming that 6KApoEp and apoE physically associate with N-terminal APP, and 6KApoEp reduced this association.

6KApoEp Reduces Aβ Production by Blocking apoE Interaction With N-Terminal Region of APP

Because 6KApoEp reduced apoE- and ApoEp-mediated Aβ production (Figure 1) as well as the physical association of apoE with N-terminal APP (Figure 2 and Supplemental

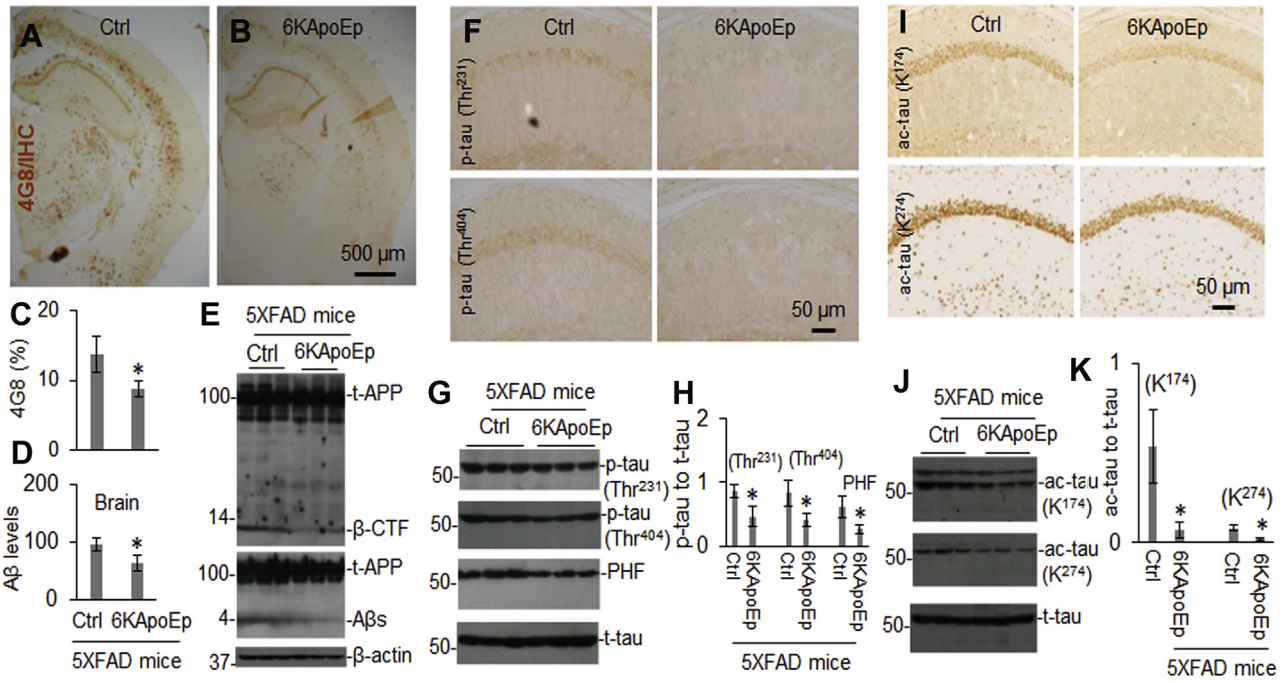

Figure 7. Peripheral administration of apolipoprotein E antagonist (6KApoEp) markedly reduces β-amyloid- and tau-associated pathology. **(A, B)** 5XFAD mice (n = 10; 5 female and 5 male) at 6 weeks of age were treated with 6KApoEp at 250 μg/kg or vehicle control (Ctrl; phosphate-buffered saline alone) intraperitoneally daily for 12 weeks, followed by analysis of β-amyloid plaques in brain tissue coronal sections by immunohistochemistry (IHC) analysis using 4G8 (upper panels). **(C)** Percentage of amyloid-β (Aβ) immunoreactive plaques in hippocampus and cortex was quantified by densitometry analysis. **(D, E)** In addition, $Aβ_{1-40,42}$ levels in brain homogenates were analyzed by enzyme-linked immunosorbent assay **(D)**, and total amyloid precursor protein (t-APP), β-C-terminal fragment (β-CTF), and soluble Aβ (Aβs) were determined in brain homogenates by Western blot analysis using 6E10 (t-APP and β-CTF) and 82E1 (t-APP and Aβs) **(E)**. **(F–K)** Phosphorylated tau (p-tau; Thr^{231} and Thr^{404}) and acetylated tau (ac-tau; K^{174} and K^{274}) were also determined by IHC **(F, I)** and Western blot analyses **(G, J)**, and band density ratios of acetylated or phosphorylated tau to total tau were determined by densitometry analysis **(H, K)**. Enzyme-linked immunosorbent assay results and band density ratios are represented as the mean ± SD. Asterisk indicates $p < .05$ vs. Ctrl. PHF, paired helical filament.

Figure S2), we wished to further investigate whether apoE LDLR binding domain interaction with N-terminal APP mediates Aβ production. Conditioned media collected from CHO/APPwt cells transiently coexpressing human wild-type apoE4 (CHO/APPwt/ApoEwt) cells, truncated apoE4 lacking the LDLR binding domain (CHO/APPwt/ApoEtrun) cells, or control vector cells were immunoprecipitated with pN-APP followed by WB analysis of apoE and secreted APP. ApoEwt but not ApoEtrun was coimmunoprecipitated with secreted APP, confirming interaction of apoE with N-terminal APP via its LDLR binding domain (Figure 3A). As confirmation, ApoEwt but not ApoEtrun was colocalized with N-terminal APP, as determined by IF staining (Figure 3C). In addition, CHO/APPwt/ApoEwt cells produced markedly more Aβ than CHO/APPwt/ApoEtrun or control vector cells. 6KApoEp reduced Aβ production in CHO/APPwt/ApoEwt cells, and ApoEp enhanced Aβ production in CHO/APPwt/ApoEtrun cells, while conditioned media collected from CHO/APPwt/ApoEwt cells but not CHO/APPwt/ApoEtrun cells increased Aβ production in CHO/APPwt cells (Figure 3B). Thus, the apoE binding domain is required for apoE association with N-terminal APP- and apoE-mediated Aβ production.

To confirm that apoE binding domain mediates Aβ production by interaction with the N-terminal region of APP, CHO/APPwt cells were treated with apoE3, apoE4, or ApoEp in the absence or presence of 22C11 or 6H3B5 antibodies. 22C11 and 6H3B5 antibodies reduced apoE3-, apoE4-, and ApoEp-mediated Aβ production in cultured cells in a dose-dependent fashion (Figure 4A and Supplemental Figure S4). In addition, CHO/APPwt cells and CHO cells expressing truncated APP lacking the N-terminal E1 region (CHO/APPdE1 cells) were treated with 6KApoEp, ApoEp, apoE3, or apoE4 followed by analysis of Aβ production. CHO/APPdE1 cells produced markedly less Aβ production compared with CHO/APPwt cells after treatment with ApoEp, apoE3, or apoE4 (Figure 4B, lower panel). In contrast, CHO/APPwt and CHO/APPdE1 cells elicited similar spontaneous Aβ production in the absence of apoE, and 6KApoEp reduced Aβ production elicited by CHO/APPwt cells but not CHO/APPdE1 cells. Therefore, apoE and ApoEp increase Aβ production and 6KApoEp reduces Aβ production by binding to the N-terminal E1 region of APP, but this region of APP is not required for spontaneous Aβ release in the absence of apoE.

6KApoEp Inhibits Cell Surface APP Trafficking and p44/42 MAPK Phosphorylation

Under physiological conditions, APP is known to be synthesized in the endoplasmic reticulum and trafficked via the trans-Golgi network to the plasma membrane, where

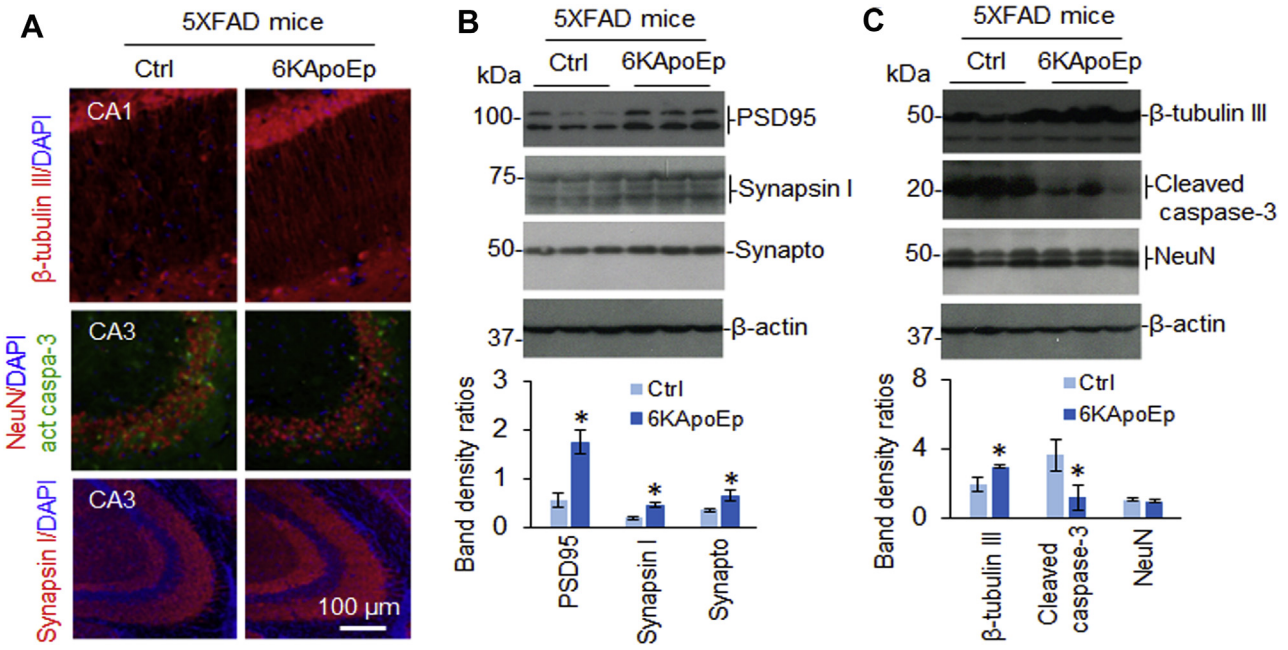

Figure 8. Peripheral administration of apolipoprotein E antagonist (6KApoEp) significantly increases presynaptic synaptophysin and postsynaptic PSD95 protein expression. 5XFAD mice (n = 10; 5 female and 5 male) at 6 weeks of age were treated with 6KApoEp at 250 μg/kg or vehicle control (Ctrl; phosphate-buffered saline alone) intraperitoneally daily for 12 weeks, followed by analysis of neurogenesis in brain tissue coronal sections by immunohistochemistry and immunofluorescence. Neuronal (β-tubulin III, neuronal nuclei [NeuN], and synapsin I), presynaptic synaptophysin (synapto), postsynaptic PSD95, and apoptotic cleaved caspase-3 were determined in brain tissue coronal sections by immunofluorescence staining **(A)** and in brain homogenates by Western blot analysis [upper panels in **(B, C)**]. Band density ratio of each protein to β-actin was determined by densitometry analysis [lower panels in **(B, C)**]. Western blot band density ratios are represented as the mean ± SD. Asterisk indicates $p < .05$ vs. Ctrl. DAPI, 4′,6-diamidino-2-phenylindole.

approximately 90% of it is cleaved by members of a disintegrin and metalloproteinase domain–containing protein (α-secretase), yielding a membrane-bound α-C-terminal APP fragment and secreted sAPPα (36). The remaining unprocessed APP (~10%) can be cleaved at the plasma membrane or further trafficked back into the cell by endocytosis, followed by cleavage by β-site APP-converting enzyme 1 (β-secretase), yielding β-C-terminal fragment (β-CTF) and sAPPβ, and by γ-secretase, ultimately generating Aβ peptides that can then be secreted from the cell (37–39). Because α-secretase cuts APP within the Aβ region, increasing Aβ generation via the endocytic pathway precludes sAPPα production. We hypothesized that decreased Aβ generation by 6KApoEp might result from decreased membrane APP trafficking and subsequent amyloidogenic processing. To test this hypothesis, we investigated the effects of apoE4 and 6KApoEp on sAPPα and Aβ production into the media as well as β-CTF and total APP levels in the plasma membrane.

CHO/APPwt cells treated with apoE4 markedly increased Aβ and β-CTF levels while reducing sAPPα levels, presumably by enhancing APP endocytosis (Figure 5A–C). Indeed, apoE4 enhanced Aβ and β-CTF levels much more in CHO/APPwt cells compared with CHO/APPswe cells, which is a better substrate for β-site APP-converting enzyme 1 and directly processed to Aβ prior to its trafficking to the cell surface (Supplemental Figure S8). In contrast, 6KApoEp reduced both basal and, more profoundly, apoE4-induced production of Aβ, β-CTF, and sAPPα without altering total APP levels, suggesting that 6KApoEp inhibits an early stage of APP processing such as the initial trafficking of APP to the plasma membrane. As further confirmation, 6KApoEp reduced both basal and apoE4-mediated cell surface APP levels, as determined by WB, flow cytometry, and confocal microscopy, regardless of whether the cells were cotreated with 6KApoEp and apoE4, pretreated with 6KApoEp, or treated with apoE4 preincubated with 6KApoEp (Figure 5D–G and Supplemental Figure S3B). 6KApoEp also reduced Aβ and β-CTF levels more in CHO/APPwt cells than in CHO/APPswe cells, consistent with reduction of APP trafficking to the cell surface (Supplemental Figure S8). Notably, apoE4 and 6KApoEp, in the absence or presence of β- or γ-secretase inhibitor, did not alter cell surface protein levels of LDLR or LRP1 as well as messenger RNA levels of APP or LDLR, suggesting that apoE and 6KApoEp do not alter APP, LDLR, and LRP1 expression or recycling (Figure 5D and Supplemental Figures S9 and S10).

Previously, apoE-mediated APP transcription/translation and Aβ production were found to be mediated by activation of a noncanonical p44/42 MAPK (29). To determine whether apoE- and ApoEp-mediated APP trafficking and processing might also be mediated by this signaling pathway, we determined the effects of apoE, ApoEp, and 6KApoEp on p44/42 and p38 MAPK phosphorylation. While ApoEp, apoE3, and apoE4 activated both p44/42 and p38 MAPK phosphorylation, 6KApoEp activated only p38 MAPK phosphorylation and inhibited apoE-induced p44/42 phosphorylation (Figure 5H

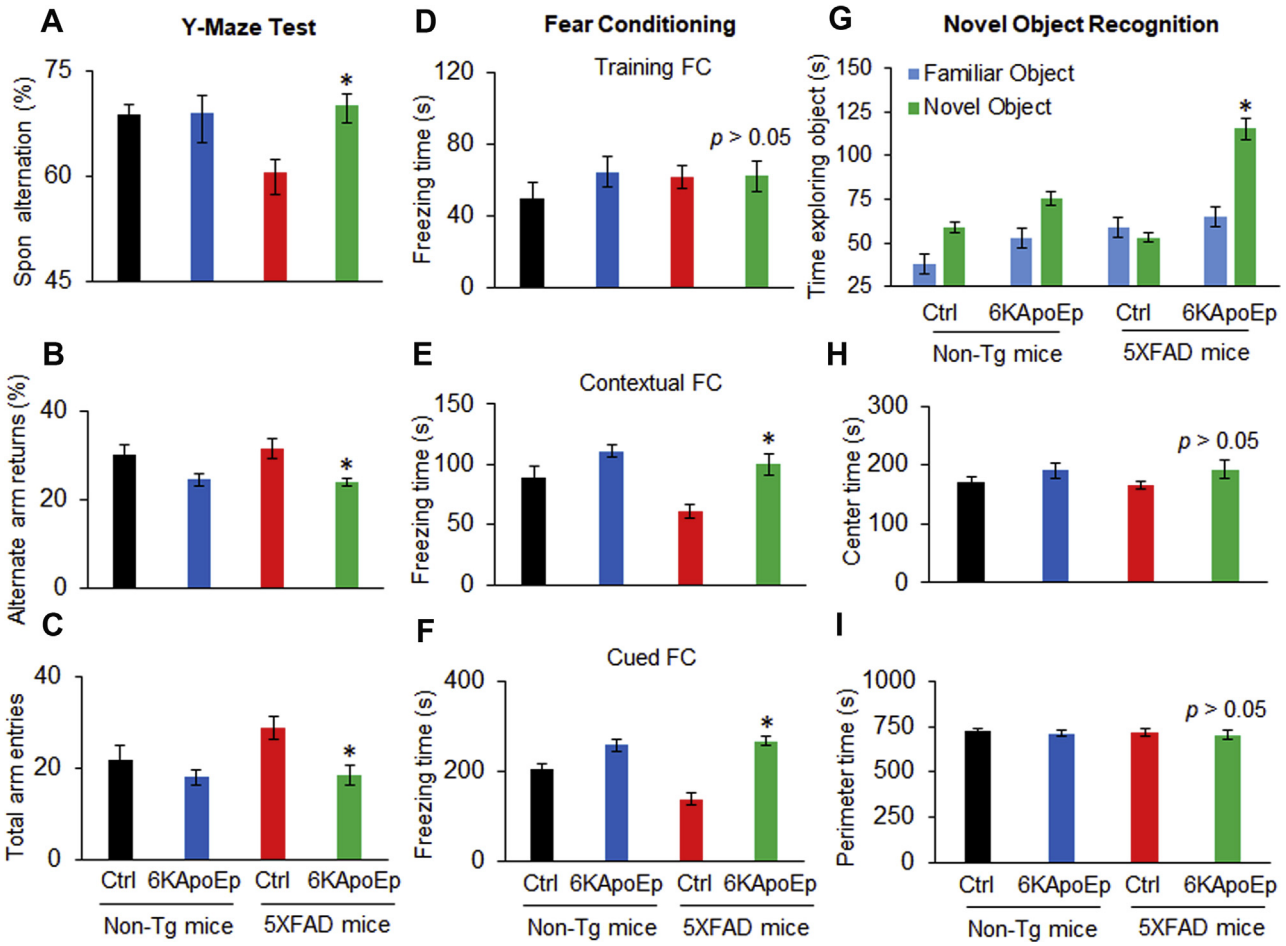

Figure 9. Apolipoprotein E antagonist (6KApoEp) treatment improves hippocampal-dependent learning and memory in 5XFAD mice. **(A–C)** Cognitive function and anxiety were determined after treatment of 5XFAD and nontransgenic control mice (n = 10; 5 female and 5 male) with 6KApoEp or vehicle phosphate-buffered saline (Ctrl). Spontaneous (Spon) alternation, alternate arm returns, and total arm entries were determined for the Y-maze testing. **(D–F)** Total freezing times during the training and contextual and cued testing after the training were determined for the fear condition (FC) testing. **(G–I)** In addition, total times exploring familiar and novel objects were determined for the novel object recognition testing **(G)**, and total times exploring central and peripheral zones were determined for the open field testing **(H, I)**. 5XFAD mice exhibited impaired cognitive functioning, as shown by reduced spontaneous alternation, freezing in the context and cued testing, and ability to discriminate between novel and familiar objects compared with nontransgenic mice, which was reversed by 6KApoEp treatment. 5XFAD mice or treatment with 6KApoEp did not exhibit altered anxiety, as determined by time spent in the center or perimeter of the open field test. Data are presented as the mean ± SD. Asterisk indicates $p < .05$ as determined by analysis of variance.

and Supplemental Figure S5). Taken together, our findings suggest that ApoEp, apoE4, and 6KApoEp may have different effects on APP processing, with ApoEp and apoE4 enhancing, and 6KApoEp reducing, cell surface APP trafficking, APP endocytosis, and amyloidogenic processing, potentially mediated by differential activation of MAPK pathways.

6KApoEp Reduces Cerebral β-Amyloid and Tau Pathologies and Memory Impairment in AD Mouse Models

Because 6KApoEp inhibits apoE-APP receptor–mediated Aβ generation, we examined whether this apoE antagonist could reduce AD-like pathology in 5XFAD mice, known to develop extensive and aggressive β-amyloid neuropathology. In addition, we examined whether mimicking the function of apoE by treatment with ApoEp could accelerate AD-like pathologies in 3XTg-AD mice, where Aβ seeding might play role in accelerating the progression of tau neuropathology. These mice were treated with ApoEp or 6KApoEp by intraperitoneal injection for 12 weeks and then euthanized, followed by analysis of cerebral Aβ and tau pathologies. Peripheral treatment of 3XTg-AD mice with ApoEp increased β-amyloid plaques, as visualized by IHC with 4G8 antibody, in comparison with mice treated with PBS as control (Figure 6A–C). Correspondingly, ApoEp increased levels of soluble $A\beta_{1-40,42}$ and β-CTF, as determined by enzyme-linked immunosorbent assay and WB analysis (Figure 6D, E), as well as levels of acetylated and phosphorylated tau, as evidenced by IHC and WB analyses (Figure 6F–K and Supplemental Figure S6). In contrast, 6KApoEp treatment reduced β-amyloid plaques, Aβ, and β-CTF levels (Figure 7A–E and Supplemental Figure S7) as

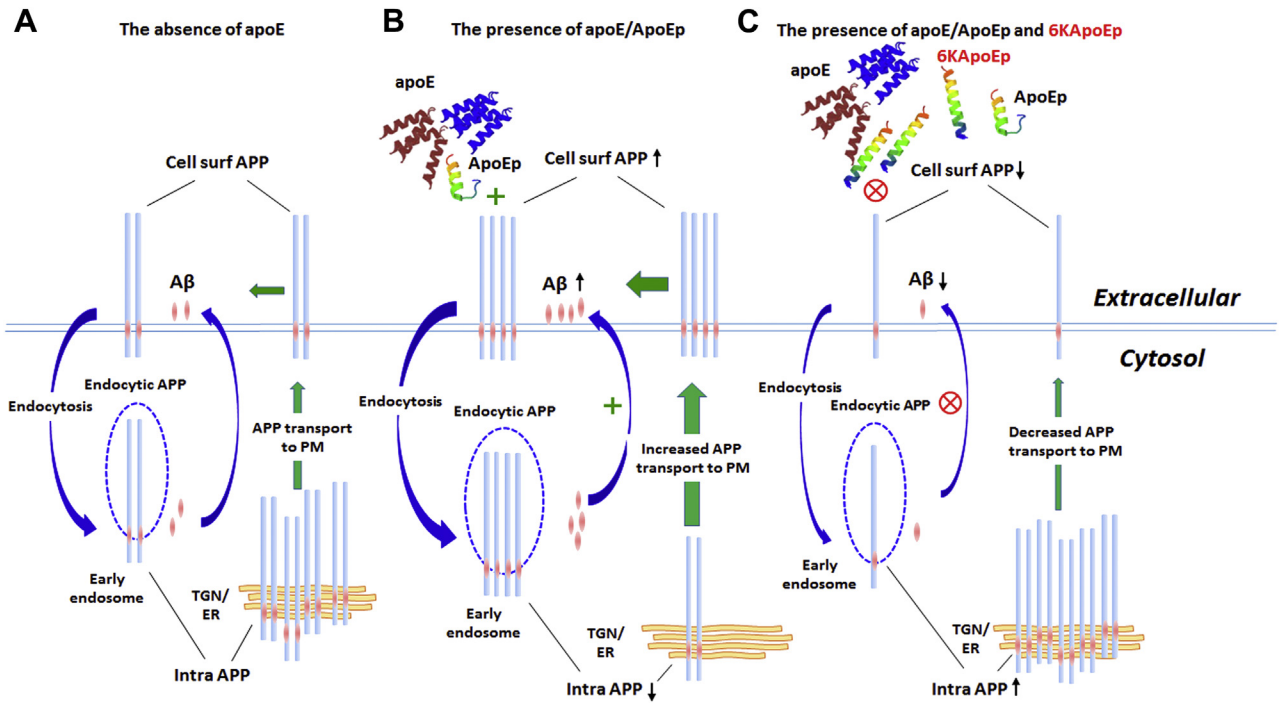

Figure 10. Schematic illustration of a novel apolipoprotein E (apoE) antagonist (6KApoEp) functionally blocking apoE or apoE low-density lipoprotein receptor binding domain peptide (ApoEp) interaction with N-terminal amyloid precursor protein (APP) and inhibiting amyloid-β (Aβ) generation by reducing APP trafficking from the trans-Golgi network (TGN) and endoplasmic reticulum (ER) to the plasma membrane (PM). **(A)** Under physiological conditions, cell surface APP (Cell surf APP) autointernalizes into the cells via clathrin-mediated vesicles, but β-site amyloid precursor protein cleaving enzyme 1 internalizes via the ADP-ribosylation factor 6–mediated endocytic pathway. APP β-cleavage occurs when lateral compartmentalization of APP and β-site amyloid precursor protein cleaving enzyme 1 meet in the early endosome at low pH and after additional γ-secretase cleavage generates Aβ, which can be secreted from the cell. In addition, newly synthesized APP travels through the secretory pathway from the ER to the PM via the TGN. **(B)** ApoE and/or ApoEp interaction with N-terminal APP increase Aβ generation by promoting internalization of APP via the endocytic pathway. In addition, binding of apoE and/or ApoEp with N-terminal APP markedly increases the trafficking of APP from the ER and TGN to the PM, as evidenced by increased cell surface APP and decreased intracellular APP (Intra APP). **(C)** 6KApoEp inhibits apoE and/or ApoEp physical interaction with N-terminal APP, which decreases APP endocytosis and trafficking from the ER and TGN to the PM, as evidenced by decreased cell surface and increased intracellular APP, reducing both secreted APPα and Aβ generation.

well as phosphorylated and acetylated tau in 5XFAD mice (Figure 7F–K). In addition, 6KApoEp treatment enhanced synaptogenesis (presynaptic synapsin I and synaptophysin and postsynaptic PSD95) and reduced neuronal apoptosis (cleaved caspase-3) (Figure 8).

In addition to determination of Aβ and tau pathologies, the effect of 6KApoEp on AD-like hippocampus-dependent learning and memory impairment was determined in 5XFAD mice using the Y maze, fear conditioning, and novel object recognition tests. Untreated 5XFAD mice exhibited learning and memory impairment compared with nontransgenic control mice, as determined by reduced spontaneous alternation in the Y maze test, which was reversed by 6KApoEp treatment (Figure 9A). 6KApoEp treatment also reduced alternate arm entry returns in both 5XFAD and nontransgenic control mice (Figure 9B). Likewise, learning impairment in 5XFAD mice was exhibited by reduced freezing times during contextual and cued testing after fear conditioning (Figure 9E, F) and reduced ability to discriminate between familiar and novel objects (Figure 9G), all of which were reversed on treatment with 6KApoEp. Notably, 5XFAD mice exhibited some hyperactivity, as shown by enhanced total arm entries in the Y maze, which was reversed by 6KApoEp treatment (Figure 9C). However, 5XFAD and nontransgenic mice, whether untreated or treated with 6KApoEp, exhibited similar levels of anxiety because they spent similar amounts of time in central and peripheral zones of the open field (Figure 9H, I). Overall, these results confirm that while apoE accelerates Aβ and tau pathologies, antagonizing the effect of apoE by 6KApoEp reduces AD-like pathology, learning impairment, and hyperactivity in an AD mouse model.

DISCUSSION

In the current study, we explored the interaction of apoE with the N-terminal region of APP as a novel therapeutic target for AD. Based on previous studies suggesting that this interaction may enhance Aβ production (28,29), we initially focused on the apoE LDLR binding domain, represented by ApoEp. We found that, like apoE, ApoEp also interacts with N-terminal APP and dose-dependently increases Aβ production (Figures 1 and 2). Antibodies against the N-terminal region of APP or the LDLR binding domain of apoE and truncation of the N-terminal domain of APP reduced apoE- and ApoEp-mediated Aβ production (Figures 3 and 4). Thus, the apoE LDLR binding domain increases Aβ production by interacting with the

N-terminal APP. Moreover, 6KApoEp, the addition of lysine residues to the N-terminal apoE, inhibited apoE- and ApoEp-mediated Aβ production, presumably through decreasing apoE–N-terminal APP interaction, APP cellular membrane trafficking, and p44/42 MAPK phosphorylation (Figures 5 and 10).

Based on our findings in vitro, we further investigated the potential of 6KApoEp as a therapeutic agent for the treatment of AD-like pathology in AD mouse models. While ApoEp enhanced $A\beta_{1-40,42}$ levels and β-amyloid plaque as well as acetylated and phosphorylated tau in 3XTg-AD mice (Figure 6), 6KApoEp reduced AD-like pathology in 5XFAD mice, reducing β-amyloid plaques, acetylated and phosphorylated tau, apoptosis, and neuroinflammation while enhancing synaptogenesis and improving hippocampus-dependent learning and memory functions (Figures 7–9 and Supplemental Figure S11). In addition, 6KApoEp presumably elicited its therapeutic effects without altering cholesterol homeostasis (Supplemental Figure S12). Taken together, these findings point to the potential of 6KApoEp as a viable therapeutic agent for the treatment of AD pathology and behavioral impairment.

Our study suggests that 6KApoEp reduces AD-like pathology by interfering with the physical interaction of apoE with N-terminal APP. Based on our findings, we suggest that apoE might have a dual function in the brain by 1) mediating cholesterol transport into the neuron and thereby promoting neuronal proliferation, differentiation, and health (18,19) and 2) binding to N-terminal APP and thereby promoting APP amyloidogenic proteolysis and resultant AD-like pathology (28,29). While the cholesterol transporting role of apoE may function well in the young and healthy brain, the APP proteolytic role of apoE might be expected to be a function of aging and disease. This hypothesis is also based on recent findings that APP has a receptor function like other type 1 transmembrane receptors that either mediates axon guidance, synaptogenesis, and growth factor signaling or mediates AD pathogenesis, depending on the environment (40–44). For example, overstimulation of APP by apoE might lead to overactivation of Go protein and APP intercellular domain, which can be pathogenic. In addition, other factors such as apoE lipidation, glycosylation, and oxidation could play a role in determining how apoE functions. Clearly, the interaction of apoE with N-terminal APP as a therapeutic target for AD should be further explored.

Lastly, our novel apoE antagonist 6KApoEp might be expected to be particularly beneficial for patients with AD who are apoE4 carriers as well as those carrying apoE3. Both apoE3 and apoE4 have a much stronger binding affinity to their receptors compared with apoE2 (45), and individuals carrying the lower-affinity apoE2 are protected against AD and have much less accumulation of β-amyloid pathology in the brain as they age (46,47). Clinically, older apoE2 carriers display superior verbal learning abilities, better recall memory, faster processing of information, and better test performance (47). 6KApoEp may specifically counteract the adverse effects of apoE4 by dampening its binding to receptors. A better understanding of the role of apoE isoforms in neuroplasticity and AD as well as their interaction with N-terminal APP and molecular mechanisms may reveal novel approaches for extending brain health span.

ACKNOWLEDGMENTS AND DISCLOSURES

This work was supported by the National Institutes of Health (Grant Nos. R01AG050253, R01AT007411, and R21AG049477 [to JTa]). This work was supported in part by the National Institute on Aging Intramural Research Program.

DS and JTa designed all experiments; DS, HH, AH, AF, JTi, and JZ carried out all experiments except for IHC and IF analyses (AH and TM); DS, HH, and JTi conducted statistical analysis of the data; JTa supervised the project; DS and JTa wrote the manuscript; and MPM, TM, AH, BG, and PRS critically edited the manuscript.

We thank Li Gan (Gladstone Institutes) for kindly providing us with monoclonal antibodies against acetylated tau (lysine^{174} and lysine^{274}). We thank Song Li for his assistance in the depiction of Figure 10, Yang Xiang and Song Li for their critical discussion, and Jared Ehrhart for his technical support in IHC and IF image analyses. Finally, we specifically thank Gobinda Sarkar for his critical discussion in designing apoE LDLR binding domain peptides.

JTa, DS, HH, and AH are inventors on a patent application submitted by the University of South Florida (Tan J, Sawmiller D, Hou H, and Habib A. US patent application 16,180,461. November 5, 2018). All other authors report no biomedical financial interests or potential conflicts of interest.

ARTICLE INFORMATION

From the Department of Psychiatry and Behavioral Neurosciences (DS, AH, HH, AF, JTi, JZ, JTa), Neuroimmunology Laboratory (BG), Department of Psychiatry and Behavioral Neurosciences, and Department of Neurosurgery and Brain Repair (PRS), Center of Excellence for Aging and Brain Repair, Morsani College of Medicine, University of South Florida, Tampa, Florida; Laboratory of Neurosciences (MPM), National Institute on Aging Intramural Research Program, and Department of Neuroscience (MPM), Johns Hopkins University School of Medicine, Baltimore, Maryland; and Departments of Biomedical Sciences and Pathology (TM), Saitama Medical Center and Saitama Medical University, Kawagoe, Saitama, Japan.

DS, AH, and HH contributed equally to this work.

Address correspondence to Jun Tan, M.D., Ph.D., Department of Psychiatry and Behavioral Neurosciences, Morsani College of Medicine, University of South Florida, Tampa, FL 33613; E-mail: jtan@health.usf.edu.

Received Nov 26, 2018; revised Mar 21, 2019; accepted Apr 15, 2019.

Supplementary material cited in this article is available online at https://doi.org/10.1016/j.biopsych.2019.04.026.

REFERENCES

1. Glenner GG, Wong CW (1984): Alzheimer's disease: Initial report of the purification and characterization of a novel cerebrovascular amyloid protein. Biochem Biophys Res Commun 120:885–890.
2. Grundke-Iqbal I, Iqbal K, Tung YC, Quinlan M, Wisniewski HM, Binder LI (1986): Abnormal phosphorylation of the microtubule-associated protein tau (tau) in Alzheimer cytoskeletal pathology. Proc Natl Acad Sci U S A 83:4913–4917.
3. Selkoe DJ (2001): Alzheimer's disease: Genes, proteins, and therapy. Physiol Rev 81:741–766.
4. Hardy J, Selkoe DJ (2002): The amyloid hypothesis of Alzheimer's disease: Progress and problems on the road to therapeutics. Science 297:353–356.
5. Schenk DB, Rydel RE, May P, Little S, Panetta J, Lieberburg I, *et al.* (1995): Therapeutic approaches related to amyloid-β peptide and Alzheimer's disease. J Med Chem 38:4141–4154.
6. Selkoe DJ, Yamazaki T, Citron M, Podlisny MB, Koo EH, Teplow DB, *et al.* (1996): The role of APP processing and trafficking pathways in the formation of amyloid β-protein. Ann N Y Acad Sci 777:57–64.
7. LaFerla FM, Tinkle BT, Bieberich CJ, Haudenschild CC, Jay G (1995): The Alzheimer's Aβ peptide induces neurodegeneration and apoptotic cell death in transgenic mice. Nat Genet 9:21–30.
8. Loo DT, Copani A, Pike CJ, Whittemore ER, Walencewicz AJ, Cotman CW (1993): Apoptosis is induced by β-amyloid in cultured central nervous system neurons. Proc Natl Acad Sci U S A 90:7951–7955.

9. Bradt BM, Kolb WP, Cooper NR (1998): Complement-dependent proinflammatory properties of the Alzheimer's disease β-peptide. J Exp Med 188:431–438.
10. Suo Z, Tan J, Placzek A, Crawford F, Fang C, Mullan M (1998): Alzheimer's β-amyloid peptides induce inflammatory cascade in human vascular cells: The roles of cytokines and CD40. Brain Res 807:110–117.
11. Hensley K, Carney JM, Mattson MP, Aksenova M, Harris M, Wu JF, *et al.* (1994): A model for β-amyloid aggregation and neurotoxicity based on free radical generation by the peptide: Relevance to Alzheimer disease. Proc Natl Acad Sci U S A 91:3270–3274.
12. Murakami K, Irie K, Ohigashi H, Hara H, Nagao M, Shimizu T, *et al.* (2005): Formation and stabilization model of the 42-mer Aβ radical: Implications for the long-lasting oxidative stress in Alzheimer's disease. J Am Chem Soc 127:15168–15174.
13. Lee VM, Trojanowski JQ (2006): Progress from Alzheimer's tangles to pathological tau points towards more effective therapies now. J Alzheimers Dis 9:257–262.
14. Rocca WA, Amaducci LA, Schoenberg BS (1986): Epidemiology of clinically diagnosed Alzheimer's disease. Ann Neurol 19:415–424.
15. Elias MF, Elias PK, Sullivan LM, Wolf PA, D'Agostino RB (2003): Lower cognitive function in the presence of obesity and hypertension: The Framingham Heart Study. Int J Obes Relat Metab Disord 27:260–268.
16. Kapogiannis D, Mattson MP (2011): Disrupted energy metabolism and neuronal circuit dysfunction in cognitive impairment and Alzheimer's disease. Lancet Neurol 10:187–198.
17. Eisenstein M (2011): Genetics: Finding risk factors. Nature 475:S20–S22.
18. Mahley RW (1988): Apolipoprotein E: Cholesterol transport protein with expanding role in cell biology. Science 240:622–630.
19. Mahley RW, Weisgraber KH, Huang Y (2009): Apolipoprotein E: Structure determines function, from atherosclerosis to Alzheimer's disease to AIDS. J Lipid Res 50(suppl):S183–S188.
20. Castellano JM, Kim J, Stewart FR, Jiang H, DeMattos RB, Patterson BW, *et al.* (2011): Human apoE isoforms differentially regulate brain amyloid-β peptide clearance. Sci Transl Med 3:89ra57.
21. Ye S, Huang Y, Mullendorff K, Dong L, Giedt G, Meng EC, *et al.* (2005): Apolipoprotein (apo) E4 enhances amyloid β peptide production in cultured neuronal cells: ApoE structure as a potential therapeutic target. Proc Natl Acad Sci U S A 102:18700–18705.
22. Harris FM, Brecht WJ, Xu Q, Tesseur I, Kekonius L, Wyss-Coray T, *et al.* (2003): Carboxyl-terminal-truncated apolipoprotein E4 causes Alzheimer's disease-like neurodegeneration and behavioral deficits in transgenic mice. Proc Natl Acad Sci U S A 100:10966–10971.
23. Brecht WJ, Harris FM, Chang S, Tesseur I, Yu GQ, Xu Q, *et al.* (2004): Neuron-specific apolipoprotein E4 proteolysis is associated with increased tau phosphorylation in brains of transgenic mice. J Neurosci 24:2527–2534.
24. Wang C, Najm R, Xu Q, Jeong DE, Walker D, Balestra ME, *et al.* (2018): Gain of toxic apolipoprotein E4 effects in human iPSC-derived neurons is ameliorated by a small-molecule structure corrector. Nat Med 24:647–657.
25. Shi Y, Yamada K, Liddelow SA, Smith ST, Zhao L, Luo W, *et al.* (2017): ApoE4 markedly exacerbates tau-mediated neurodegeneration in a mouse model of tauopathy. Nature 549:523–527.
26. Uddin MS, Kabir MT, Al Mamun A, Abdel-Daim MM, Barreto GE, Ashraf GM (2019): APOE and Alzheimer's disease: Evidence mounts that targeting APOE4 may combat Alzheimer's pathogenesis. Mol Neurobiol 56:2450–2465.
27. Zhao N, Liu CC, Qiao W, Bu G (2018): Apolipoprotein E, receptors, and modulation of Alzheimer's disease. Biol Psychiatry 83:347–357.
28. Hass S, Fresser F, Kochl S, Beyreuther K, Utermann G, Baier G (1998): Physical interaction of ApoE with amyloid precursor protein independent of the amyloid Aβ region in vitro. J Biol Chem 273:13892–13897.
29. Huang YA, Zhou B, Wernig M, Sudhof TC (2017): ApoE2, ApoE3, and ApoE4 differentially stimulate APP transcription and Aβ secretion. Cell 168:427–441.e421.
30. Rezai-Zadeh K, Shytle D, Sun N, Mori T, Hou H, Jeanniton D, *et al.* (2005): Green tea epigallocatechin-3-gallate (EGCG) modulates amyloid precursor protein cleavage and reduces cerebral amyloidosis in Alzheimer transgenic mice. J Neurosci 25:8807–8814.
31. Obregon D, Hou HY, Deng J, Giunta B, Tian J, Darlington D, *et al.* (2012): Soluble amyloid precursor protein-α modulates β-secretase activity and amyloid-β generation. Nat Commun 3:777.
32. Zhu Y, Hou H, Rezai-Zadeh K, Giunta B, Ruscin A, Gemma C, *et al.* (2011): CD45 deficiency drives amyloid-β peptide oligomers and neuronal loss in Alzheimer's disease mice. J Neurosci 31:1355–1365.
33. Li S, Deng J, Hou H, Tian J, Giunta B, Wang Y, *et al.* (2014): Specific antibody binding to the APP672-699 region shifts APP processing from α- to β-cleavage. Cell Death Dis 5:e1374.
34. Sawmiller D, Li S, Mori T, Habib A, Rongo D, Delic V, *et al.* (2017): Beneficial effects of a pyrroloquinolinequinone-containing dietary formulation on motor deficiency, cognitive decline and mitochondrial dysfunction in a mouse model of Alzheimer's disease. Heliyon 3:e279.
35. Sawmiller D, Habib A, Li S, Darlington D, Hou H, Tian J, *et al.* (2016): Diosmin reduces cerebral Aβ levels, tau hyperphosphorylation, neuroinflammation, and cognitive impairment in the 3xTg-AD mice. J Neuroimmunol 299:98–106.
36. Haass C, Selkoe DJ (1993): Cellular processing of beta-amyloid precursor protein and the genesis of amyloid beta-peptide. Cell 75:1039–1042.
37. Habib A, Sawmiller D, Tan J (2017): Restoring soluble amyloid precursor protein α functions as a potential treatment for Alzheimer's disease. J Neurosci Res 95:973–991.
38. Eggert S, Thomas C, Kins S, Hermey G (2018): Trafficking in Alzheimer's disease: Modulation of APP transport and processing by the transmembrane proteins LRP1, SorLA, SorCS1c, sortilin, and calsyntenin. Mol Neurobiol 55:5809–5829.
39. Zhang X, Song W (2013): The role of APP and BACE1 trafficking in APP processing and amyloid-β generation. Alzheimers Res Ther 5:46.
40. Bukhari H, Glotzbach A, Kolbe K, Leonhardt G, Loosse C, Müller T (2017): Small things matter: Implications of APP intracellular domain AICD nuclear signaling in the progression and pathogenesis of Alzheimer's disease. Prog Neurobiol 156:189–213.
41. Copenhaver PF, Kögel D (2017): Role of APP interactions with heterotrimeric G proteins: Physiological functions and pathological consequences. Front Mol Neurosci 10:3.
42. Dawkins E, Small DH (2014): Insights into the physiological function of the β-amyloid precursor protein: Beyond Alzheimer's disease. J Neurochem 129:756–769.
43. Deyts C, Thinakaran G, Parent AT (2016): APP Receptor? To be or not to be. Trends Pharmacol Sci 37:390–411.
44. Sosa LJ, Caceres A, Dupraz S, Oksdath M, Quiroga S, Lorenzo A (2017): The physiological role of the amyloid precursor protein as an adhesion molecule in the developing nervous system. J Neurochem 143:11–29.
45. Bu G (2009): Apolipoprotein E and its receptors in Alzheimer's disease: Pathways, pathogenesis and therapy. Nat Rev Neurosci 10:333–344.
46. Benjamin R, Leake A, McArthur FK, Ince PG, Candy JM, Edwardson JA, *et al.* (1994): Protective effect of apoE ε2 in Alzheimer's disease. Lancet 344:473.
47. Suri S, Heise V, Trachtenberg AJ, Mackay CE (2013): The forgotten APOE allele: A review of the evidence and suggested mechanisms for the protective effect of APOE ε2. Neurosci Biobehav Rev 37:2878–2886.
48. Tokuda T, Calero M, Matsubara E, Vidal R, Kumar A, Permanne B, *et al.* (2000): Lipidation of apolipoprotein E influences its isoform-specific interaction with Alzheimer's amyloid β peptides. Biochem J 348:359–365.
49. Krul ES, Tang J (1992): Secretion of apolipoprotein E by an astrocytoma cell line. J Neurosci Res 32:227–238.